

Z.F. LI
B.X. LIU✉

Growth of fractal patterns during irradiation-induced amorphization in nano-sized Ni–W multilayers

Advanced Materials Laboratory, Department of Materials Science and Engineering, Tsinghua University, Beijing 100084, P.R. China

Received: 30 January 2002/Accepted: 2 February 2002
Published online: 3 May 2002 • © Springer-Verlag 2002

ABSTRACT In the Ni–W system, a uniform amorphous Ni–W phase was obtained by ion irradiation of the nano-sized Ni–W multilayers at liquid-nitrogen temperature. Interestingly, before undergoing complete amorphization, fractal patterns were observed at a relatively low irradiation dose (3×10^{14} Xe⁺/cm²), and the patterns were characterized to consist of crystalline grains of Ni-enriched solid solution. The fractal dimension was measured to be about 1.68 ± 0.05 , which was very close to that expected by the cluster diffusion-limited aggregation model.

PACS 81.05.Kf; 61.80.Hz; 61.43.Hv; 61.82.Bg

1 Introduction

In the last two decades, the scientific issue of fractals has been extensively studied. Most of the efforts were focused on the growth mechanisms of the fractal patterns, which manifest themselves in widely diverse scientific fields. It has also been shown that thin solid films seem to be a favorable environment for growing two-dimensional random patterns, e.g. fractal-like structures could be observed in sputtering-deposited thin films [1], during the crystallization of amorphous thin films [2] and in ion-irradiated amorphous films [3], etc. All the above fractal patterns were characterized with a fractal dimension of about 1.7, which can be explained by the well-known models based on diffusion-limited aggregation (DLA) [4]. Although there is an extensive literature concerning the development of unique surface morphology, only a few reports present observations of surface morphology on thin films subjected to ion-beam bombardment. In this respect, Liu et al. [3] have reported the formation of fractal pat-

terns in Ni–Mo thin films caused by 200-keV Xe-ion irradiation. Besides, Ding and Liu have reported observations of percolation networks in ion-irradiated Ag–Co solid films [5]. We present, in this Letter, some interesting patterns that emerged on the surface of Ni–W multilayers while being subjected to Xe-ion irradiation at liquid-nitrogen temperature and the possible mechanism responsible for the growth of the patterns.

2 Experimental procedure

The Ni–W multilayered films were prepared by alternate deposition of pure nickel (99.9% Ni) and tungsten (99.9% W) onto cleaved NaCl single crystals in an ultra high vacuum (UHV) e-gun evaporation system with a background vacuum level of the order of 10^{-11} Torr. During deposition, the vacuum level was better than 1.6×10^{-8} Torr. The deposition rate was controlled at 0.5 \AA/s and no special cooling was provided to the substrates during deposition. The overall composition of the films was designed

to be Ni₅₀W₅₀. For an ion beam mixing experiment, the total thickness of the films was about 40 nm, which was required to match the projected range plus projected range straggling of 200-keV Xe ions. The Ni–W multilayers were designed to consist of eight Ni and eight W layers, and the desired overall compositions of the multilayered films were obtained by adjusting the relative thicknesses of the individual Ni and W layers. After deposition, the real composition of the films was confirmed to be very close to Ni₅₀W₅₀, by energy-dispersive spectrum (EDS) analysis with a measuring error around 4%. The as-deposited films were then irradiated by 200-keV Xe ions at room temperature in an implanter with a vacuum level of 10^{-6} Torr. The Xe-ion current density was confined to be about $0.5 \mu\text{A cm}^{-2}$ to avoid an overheating effect. An as-deposited film and all the irradiated films were removed from the NaCl substrates by de-ionized water and placed onto the Cu grids for transmission electron microscopy (TEM) and selected-area diffraction (SAD) analysis. Besides, an image-processing computer was used to calculate the fractal dimension for the formed patterns observed on the films.

3 Results and discussion

Figure 1a and b show a bright-field image and corresponding SAD pattern of the as-deposited Ni₅₀W₅₀ films. In Fig. 1b, sharp diffraction lines reflected from polycrystalline Ni and W, respectively, can clearly be seen, indicating that in the as-deposited films both Ni and W were of a crystalline structure. After the Ni₅₀W₅₀ multilay-

✉ E-mail: dmslbx@tsinghua.edu.cn

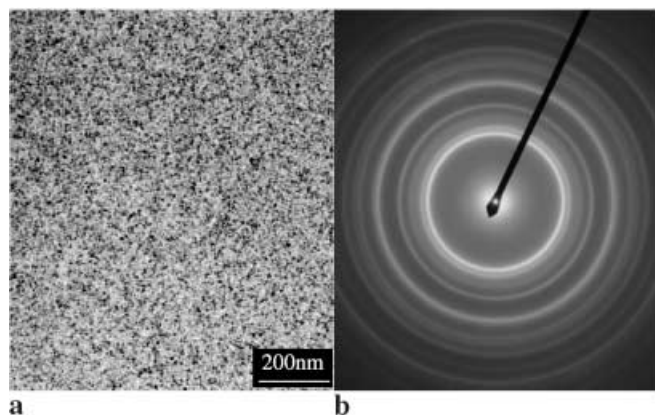


FIGURE 1 a and b are the bright-field image and the corresponding SAD pattern of the as-deposited $\text{Ni}_{50}\text{W}_{50}$ multilayered films

ered films were irradiated to a dose of $1 \times 10^{14} \text{Xe}^+/\text{cm}^2$, there was no significant change in both surface morphology and SAD patterns, which are therefore not shown here. When the irradiation dose went up to $3 \times 10^{14} \text{Xe}^+/\text{cm}^2$, TEM examination revealed some interesting features emerging on the Ni–W film surface, and some typical morphologies are shown in Fig. 2a, b and c. Obviously, one conspicuous feature of these morphologies is the discontinuity of the pattern components. Each morphology with an average size of $10 \mu\text{m}$ is composed of $0.2\text{--}2\text{-}\mu\text{m}$ particles or pattern components of dark appearance. The EDS analysis indicated that the dark particles were Ni-enriched precipitates. Furthermore, Fig. 2d and e show the corresponding SAD patterns of the particles and the matrix, respectively. From the SAD patterns, it was identified that each dark particle is a Ni-enriched single-crystalline grain (solid solution), and the matrix is an amorphous Ni–W alloy phase.

To characterize the observed patterns in a quantitative manner, a pattern was first divided into concentric disks with various radii R , and the number of pixels N (corresponding to an area occupied by the pattern) in each disk was then counted by the image-processing computer. It turned out that a linear correlation could be fitted for $\log N$ versus $\log R$, which corroborated that the surface pattern was indeed of a fractal with self-similarity, and the fractal dimension was thus obtained. Figure 3 shows the calculation results and the average fractal dimension is about 1.68 ± 0.05 .

Figure 4a and b show a bright-field image and corresponding SAD pattern

of the $\text{Ni}_{50}\text{W}_{50}$ films after ion irradiation to a dose of $5 \times 10^{14} \text{Xe}^+/\text{cm}^2$. In Fig. 4b, all the crystalline diffraction lines from W and Ni disappeared and only a few halos were observed, indi-

cating that complete amorphization was achieved in the $\text{Ni}_{50}\text{W}_{50}$ films. Besides, the bright-field image in Fig. 4a shows that the morphology of the amorphous phase is fairly uniform. In fact, the samples irradiated to doses from $5 \times 10^{14} \text{Xe}^+/\text{cm}^2$ to $7 \times 10^{15} \text{Xe}^+/\text{cm}^2$ all showed similar morphologies and diffraction patterns as those displayed in Fig. 4a and b.

We now discuss the growth process of the observed fractal aggregates. As mentioned above, when the irradiation dose went up to a critical dose, i.e. $3 \times 10^{14} \text{Xe}^+/\text{cm}^2$, fractal patterns were observed. The dose was considered to be critical, because both higher doses ($5 \times 10^{14} \text{Xe}^+/\text{cm}^2 \sim 7 \times 10^{15} \text{Xe}^+/\text{cm}^2$) and lower doses ($1 \times 10^{14} \text{Xe}^+/\text{cm}^2$) could not result in the formation of a fractal pattern. It is well known that ion irradiation can produce defects in

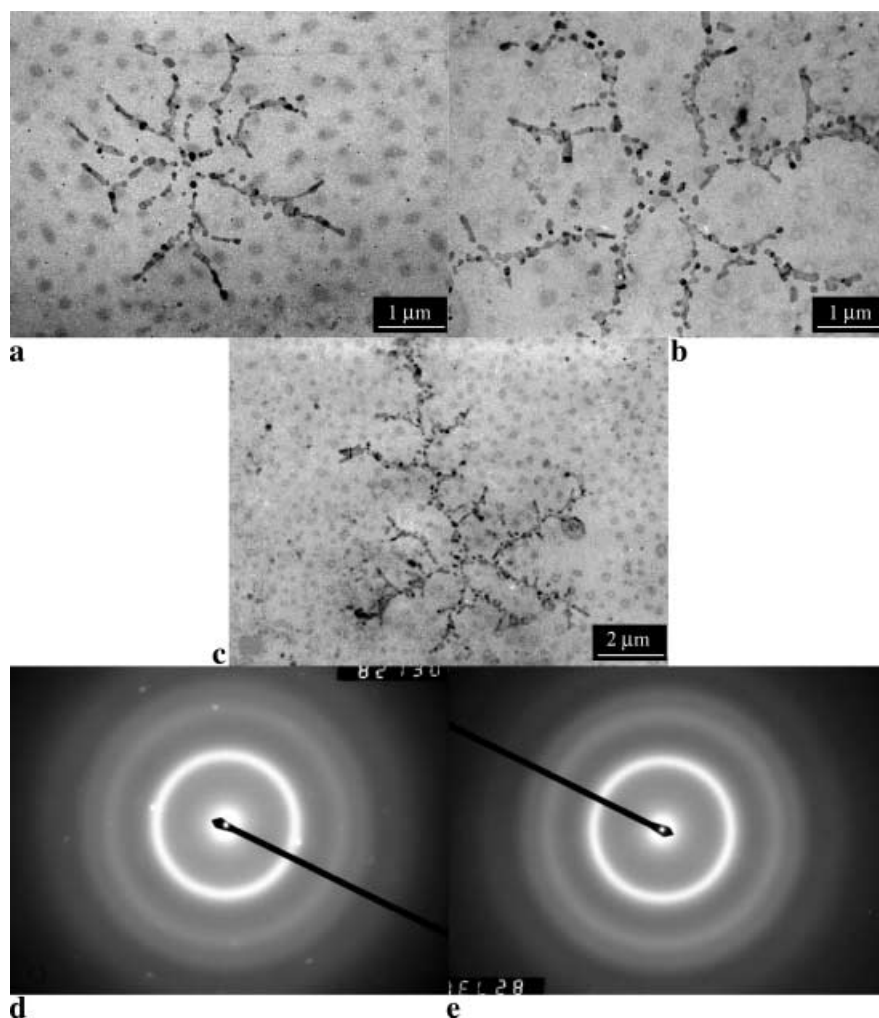


FIGURE 2 a, b and c are three typical fractal patterns which have grown on the surface of the $\text{Ni}_{50}\text{W}_{50}$ films after irradiation to a dose of $3 \times 10^{14} \text{Xe}^+/\text{cm}^2$; d and e are the SAD patterns of the particle and matrix in a, respectively

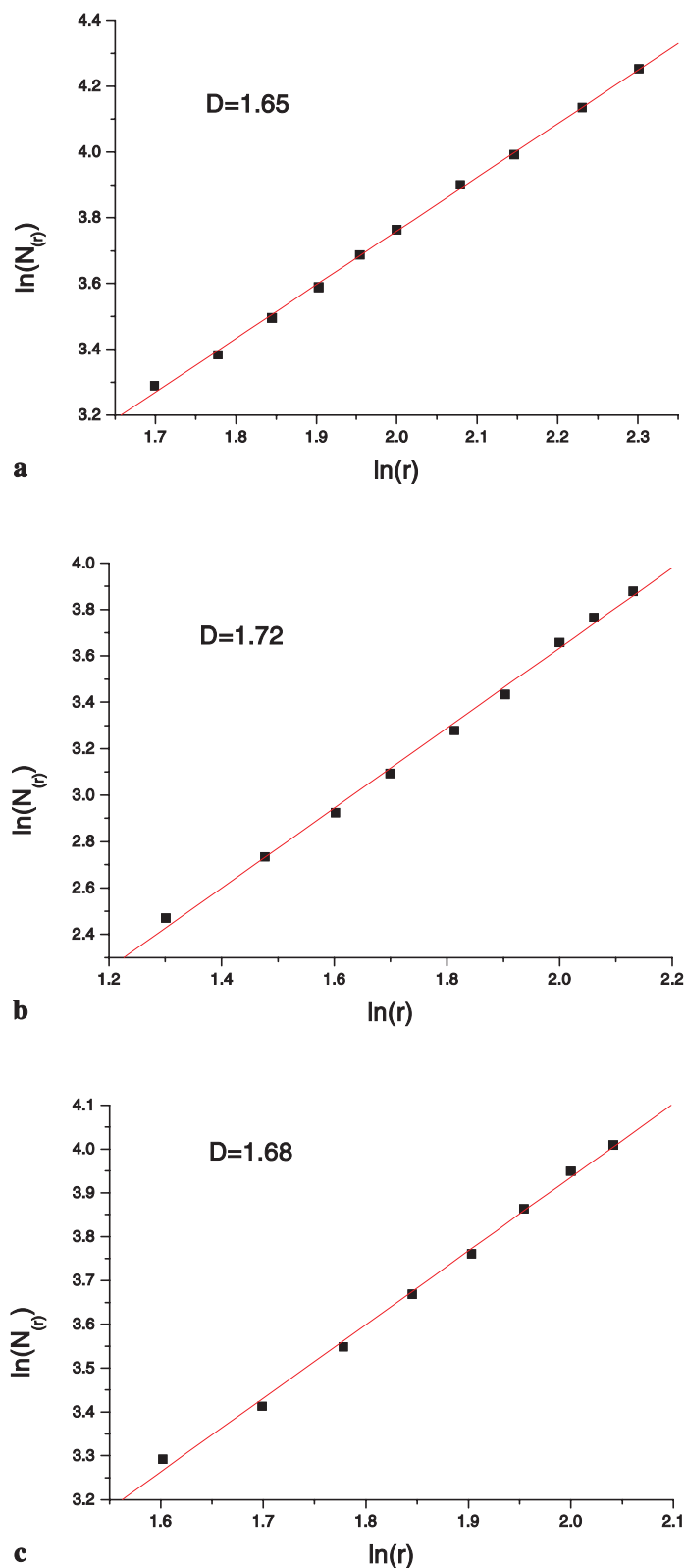


FIGURE 3 Double-logarithmic plot in the fractal analysis for the patterns shown in Fig. 2a, b, and c, respectively. The fractal dimension D is given for each plot together

thin solid films. The reason why the lower-dose irradiation could not form a fractal structure is that these doses could not produce enough defects in

the films. While, for the higher-dose irradiation, it is thought that as soon as the fractal structures were formed at the critical dose of $3 \times 10^{14} \text{ Xe}^+/\text{cm}^2$, fur-

ther irradiation would destroy the fractal structures. That is why no fractal pattern was observed after higher-dose irradiation either.

Comparing the morphologies in Fig. 1a and Fig. 2a, one finds that the particles of the fractal should not directly grow from the polycrystalline grains that have formed in the as-deposited films. Besides, noticing that the matrix of the fractal patterns is an amorphous phase, it is deduced that the fractal pattern might grow from the amorphous matrix. The amorphous structure therefore apparently plays an important role in the formation of the fractal patterns. In fact, Ben-Jacob et al. [6] showed that a dense branching morphology is generated in an annealing experiment of amorphous alloys.

It is well known that ion irradiation is a far from equilibrium process. Generally, the process can be divided into two steps, i.e. the first step is of an atomic collision cascade and the second step is of relaxation. It is commonly recognized that the structure of the newly formed alloy phase is fixed in the relaxation period, but not in the first step of atomic collision, during which a large number of atoms are in violent motion [7]. During the relaxation period, because of a very high effective cooling rate (10^{13} – 10^{14} K/s) [8], those phases with complicated structures cannot be formed, and only simple structured phases can form. It is also known that, in a given binary metallic system, the composition range favoring amorphization is limited, because formation of the solid solutions is more favored than the amorphous phase within both terminal solid-solution compositions. In the present study, after ion irradiation to a critical dose of $3 \times 10^{14} \text{ Xe}^+/\text{cm}^2$, the Ni and W layers were generally mixed together. Nonetheless, at the beginning of the relaxation period, the already mixed Ni–W films were not homogeneous everywhere in composition. In other words, in some local areas, the composition could be close to the Ni terminal solid solution due to the compositional fluctuation. As a result, during the very short relaxation period (10^{-9} – 10^{-10} s) [8], most of the mixture with an average composition of about $\text{Ni}_{50}\text{W}_{50}$ could form an amorphous phase, while in some local areas Ni-

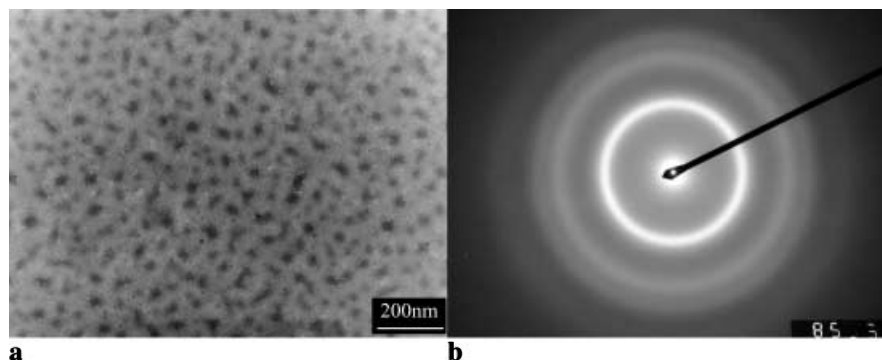


FIGURE 4 **a** and **b** are the bright-field image and the corresponding SAD pattern of the $\text{Ni}_{50}\text{W}_{50}$ films after irradiation to a dose of $5 \times 10^{14} \text{Xe}^+/\text{cm}^2$

enriched solid solutions were formed and organized themselves into a fractal pattern. Viewed in this light, the fractal patterns formed in the present study probably reflected such a growth mechanism related to an amorphous–crystal phase transition.

Coincidentally, in the present study, the dimension of the fractal patterns is 1.68 ± 0.05 , which is very close to the one expected by the cluster diffusion-limited aggregation (CDLA) model [9],

as well as to the previous results obtained in Ni–Mo thin solid films [3].

4 Conclusions

In summary, we have shown that, at a critical irradiation dose of $3 \times 10^{14} \text{Xe}^+/\text{cm}^2$, a fractal pattern could grow in nano-sized $\text{Ni}_{50}\text{W}_{50}$ multilayered films, which eventually turned into a uniform amorphous $\text{Ni}_{50}\text{W}_{50}$

phase at medium doses ranging from 5×10^{14} to $7 \times 10^{15} \text{Xe}^+/\text{cm}^2$.

ACKNOWLEDGEMENTS The financial aid from the National Natural Science Foundation, and the Ministry of Science and Technology of China (through Grant No. G2000067207) are gratefully acknowledged.

REFERENCES

- 1 W.T. Elam, S.A. Wolf, J. Sprague, D.U. Gubser, D. Van Vechten, G.L. Barz, Jr., P. Meakin: *Phys. Rev. Lett.* **54**, 701 (1985)
- 2 G. Radnoczi, T. Vicsek, L.M. Sander, D. Grier: *Phys. Rev. A* **35**, 4012 (1987)
- 3 B.X. Liu, L.J. Huang, K. Tao, C.H. Shang, H.D. Li: *Phys. Rev. Lett.* **59**, 745 (1987)
- 4 T.A. Witten, L.M. Sander: *Phys. Rev. B* **27**, 5686 (1983)
- 5 J.R. Ding, B.X. Liu: *Phys. Rev. B* **40**, 5834 (1989)
- 6 E. Ben-Jacob, G. Deutscher, P. Garik, N.D. Goldenfeld, Y. Lareah: *Phys. Rev. Lett.* **57**, 1903 (1986)
- 7 B.X. Liu, W.S. Lai, Q. Zhang: *Mater. Sci. Eng., R* **29**, 1 (2000)
- 8 M.W. Thompson: *Defects and Radiation Damage in Metals* (Cambridge University Press, Cambridge, UK 1969) Chaps. 4 and 5
- 9 R.F. Voss: *J. Statist. Phys.* **36**, 861 (1984)